Magnetic circular dichroism of the *DX* center in $Al_{0.35}Ga_{0.65}As$:Te

R. E. Peale, Y. Mochizuki,* H. Sun, and G. D. Watkins
Sherman Fairchild Laboratory 161, Lehigh University, Bethlehem, Pennsylvania 18015
(Received 20 May 1991)

Magneto-optical absorption spectra of 0.4-mm-thick, single-crystal $Al_{0.35}Ga_{0.65}As$:Te give evidence for two bleachable absorbers, one of which is identified as the *DX* center. The bleached-state absorption coefficient and magnetic circular dichroism (MCD), measured from 0.66 to 2.2 μm at 1.7 K, are adequately described by the Drude free-electron model. Cooling the sample in darkness leads to transmission transients, from which ground-state absorption coefficients and optical-conversion cross sections for the bleachable absorbers are derived. The conversion threshold is 0.6 eV for the *DX* and 1.5 eV for the second bleacher, and the recovery behavior is significantly different for the two. The MCD at the beginning of each transient is identified with the ground state of each absorber, and temperature dependence reveals that the bulk of the initial MCD has a nonparamagnetic origin. We conclude that the paramagnetic contribution to the MCD from the *DX* ground state is very small, being less than 0.004% of its peak absorption coefficient at $T=1.7$ K and $B=2$ T. This provides strong support to the diamagnetic-ground-state, negative-U model of Chadi and Chang. The origin of the second bleachable absorber has not been established.

I. INTRODUCTION

The electrical properties of $Al_xGa_{1-x}As$ doped with the conventional substitutional group-IV (Si,Ge,Sn) or group-VI (S,Se,Te) donors are observed to change abruptly in the compensation region $x>0.22$.[1,2] For $x<0.22$, the donors are characterized by simple shallow effective-mass-like states. For $x>0.22$, a deeper state emerges into the gap, trapping and removing free carriers, and dominating the electrical properties of the material. This deep level—the so-called *DX* center—has been a subject of intense interest and controversy during the past decade. This interest stems in part from the *DX* center's influence on the performance of $Al_xGa_{1-x}As$/GaAs modulation-doped field-effect transistors, which are being developed for high-speed circuit applications.[2] More fundamentally, the *DX* phenomenon is a fascinating, challenging, and still unsolved scientific puzzle.

It is now well established[2] that *DX* centers in $Al_xGa_{1-x}As$ arise from the isolated substitutional n-type dopants and do not involve a second impurity or defect nearby as originally proposed.[3] For $x>0.22$, these group-IV or group-VI impurities introduce both the deep *DX* level and a shallow effective-mass level in the gap. (In pure GaAs, *DX* centers can be induced by hydrostatic pressure,[4] since this alters the band structure in a way similar to alloying.) The deep level's optical ionization energy is much larger than its thermal one. The shallow level can be metastably occupied below ~ 100 K by optical excitation, resulting in persistent photoconductivity (PPC). Recapture by the deep level is a thermally activated, multiphonon-emission process; optical capture does not occur. These properties appear best explained in terms of a large lattice relaxation model in which a substantial change in lattice configuration occurs in the transformation between the shallow and deep states.[1-3,5] The extent and microscopic nature of the relaxation is still in question, however. Direct experimental probes of the local distortion have yielded contradictory results.[6-13]

Recent calculations[14,15] by Chadi and Chang have produced detailed predictions for the microscopic nature of a large lattice relaxation at the *DX*. For group-IV donors, which occupy a group-III lattice site, the donor is predicted to break its bond with a nearby As neighbor and relax in the opposite $\langle 111 \rangle$ direction. For group-VI donors, which reside on group-V lattice sites, it is the nearby group-III host atom that breaks away in a $\langle 111 \rangle$ direction from the donor. A condition necessary for these relaxations to occur is that the donor bind two electrons in its relaxed state. Assuming that the available electrons come from the donors, with each donor contributing one, only half of the donors can be in the relaxed (deep) state. The other half remain as ionized shallow donors. Hence, the *DX* is predicted to behave as a negative-U system.[16] (This prediction has subsequently been duplicated for the Si atoms by Dabrowski, Scheffler, and Strehlow.[17] However, it is important to point out that in a similar calculation by Yamaguchi, Shiraishi, and Ohno,[18] this distortion was not predicted to be stable.)

The physical mechanism in the Chadi and Chang model can be viewed as a Jahn-Teller distortion of a highly localized, excited t_2 state.[19] Occupancy by one electron would be sufficient to cause the off-center state to be the lowest if the relaxational energy gain exceeded the undistorted system's ground- to excited-level promotion energy. Occupancy by two electrons doubles the Jahn-Teller coupling, and so the magnitude of the corresponding energy gain, which goes as the square of the coupling coefficient, increases fourfold. At the same time, the energy required to promote two electrons to the t_2 level has increased by only a factor of 2. However, working against this is the Coulomb repulsion energy U associated with the two electrons in the same highly localized orbit-

al. If U is not too large, given by the Anderson criterion,[20] the two-electron state is favored, and the "effective" U is negative, since the second electron is bound more strongly than the first.

Negative U is not a common phenomenon, however. In fact only twice has negative U been demonstrated for semiconductor defects with known microscopic identities, and both are in silicon.[16] Many experiments have been performed to test the DX for negative-U behavior. The most convincing so far may be divided into two general categories: those which attempt to count the number of electrons trapped by the deep DX state, and those which attempt to detect DX paramagnetism. (Diamagnetism is expected in the case of negative-U behavior since two electrons pair with opposite spins.)

In the first category, a recent measurement of the relative intensity of a pressure-induced DX Mössbauer resonance in GaAs:Sn has been cited as evidence that the DX localizes more than a single electron.[21] A similar, very recent study of the localized vibrational modes of Si in GaAs versus hydrostatic pressure also has been interpreted to indicate that DX traps two electrons.[22] In another experiment,[23] just enough hydrostatic pressure was applied to GaAs:Ge+Si, to make the Ge donor, but not the Si donor, DX like. Then, the number of electrons trapped at the deep DX state was monitored for different concentrations of Si, whose role was simply to supply electrons. The number of electrons trapped at the deep state, as monitored by deep-level transient spectroscopy and capacitance-voltage measurements, was estimated to exceed the number of DX centers, supporting again the idea that the deep DX state binds more than one electron.

In the second category, conflicting static magnetic-susceptibility measurements have been reported: one concluding that the ground state is paramagnetic,[24] another concluding that the observed paramagnetism is an order of magnitude smaller than predicted assuming equal free-spin and DX concentrations.[25] The failure[26,27] to observe spin resonance associated with the deep level is consistent with negative-U behavior, but there are always several possible reasons for failure to detect a paramagnetic defect (inhomogeneous alloy broadening, rapid spin-lattice relaxation broadening, etc.), and this also must be considered inconclusive.

Other types of experiments have provided information about the DX charge state, but the results are less convincing. For example, measurements of electron mobility, which depends on defect charge states, have been used to support different conclusions.[28,29]

Our purpose in the present work is to determine the paramagnetic contribution to magnetic circular dichroism (MCD) in the near-infrared absorption band of the deep DX state. This contribution is relatively less sensitive than EPR to the width and relaxation times of the ground Zeeman-split states and, therefore, should reflect more nearly the ground-state static susceptibility. In addition, being detected in an absorption band specific to the DX center, the measurement is defect specific. Therefore, if a paramagnetic component is detected, it should convincingly rule out negative-U properties of DX. On the other hand, if none is detected, it will represent a strong additional argument for DX negative-U properties.

MCD arises from spin-orbit interaction in the excited state involved in the optical-absorption transition.[30] Its magnitude should reflect, therefore, the atomic spin-orbit interaction of the constituent atoms in the core of the defect. For this reason, the heavier atom tellurium was selected as the DX donor in our studies. The results to be described in this paper can be summarized briefly as follows.

(1) The optical transmission of $Al_{0.35}Ga_{0.65}As$ cooled in the dark is time dependent. Cooling in darkness populates the deep ground-state levels, and the light then converts the centers to their metastable states, with the result that the initial absorption is bleached and replaced by a different absorption. From analysis of the transient change in transmission, the absorption coefficients of the ground and metastable states are separately determined and found to have different spectral dependences. The time dependence of the conversion determines the optical conversion cross section.

(2) Two distinct bleachable absorbers have been identified in our sample. The spectral dependences of the optical conversion cross section, markedly different for the two, identify one as the expected Te DX center. The metastable- to ground-state recovery kinetics also differs for the two, as determined from isochronal and isothermal annealing curves. We denote this second bleachable absorber PPC2, because it also contributes a second separable component to the persistent free carriers. To our knowledge the existence of this component has not previously been noted. We do not know its origin but we tentatively conclude that it is unrelated to the Te DX center.

(3) The MCD of $Al_{0.35}Ga_{0.65}As$ cooled in the dark is transient, too. In the bleached state, the free-electron Drude model adequately describes both the absorption coefficient and MCD, and this interpretation yields an effective-mass value in reasonable agreement with a recent, more accurate determination. The initial MCD, measured before significant bleaching has occurred, is associated with the DX and PPC2 ground states and reveals no evidence of temperature dependence. An upper limit for the paramagnetic contribution to the MCD of only 0.004% of the peak ground-state absorption at $T=1.7$ K and $B=2$ T has been inferred from the scatter of the data.

This paper is divided into five sections. Section II gives experimental details. Section III describes measurements of the metastable state absorption and MCD for both the DX and PPC2. Section IV describes the determination of the absorption coefficient and conversion cross section for the DX and PPC2, and ground-state MCD for the DX. Section IV also presents our measurements of the DX and PPC2 recovery. The summary and conclusions are presented last in Sec. V.

II. EXPERIMENTAL DETAILS

Our sample was a 0.037-cm-thick single crystal of $Al_{0.35}Ga_{0.65}As$ doped with Te. It was grown by the

liquid-phase epitaxy method on a GaAs substrate by Hitachi Cable Co. Ltd., and the Te doping level was specified as 1.2×10^{18} cm^3. The substrate was lapped off prior to our measurements.

The sample transmittance and MCD were measured with the sample immersed in liquid helium (4.2, 1.7 K) in an Oxford Spectromag-4 optical-access magnet cryostat with quartz windows. The light source was a tungsten-halogen lamp. A Jarrel-Ash Mark X, $\frac{1}{4}$-meter monochromator (600 lines/mm, 1 μm blaze grating) selected wavelength, with colored glass or semiconductor filters to eliminate unwanted orders, and an image of the output slit was focused onto the sample. The image was larger than the sample to insure uniform sample excitation. Liquid-nitrogen-cooled Ge, InSb, or InAs detectors were used to monitor the transmitted light. The spectral dependence of the incident light intensity was determined with a pyroelectric detector at the output slit of the monochromator.

The sample, mounted on a quartz rod at the end of a long stainless-steel tube, could be lifted into a warmer part of the cryostat for recovery of the deep *DX* state in the dark and then returned for further optical studies. For study of the recovery kinetics, a copper-Constantan thermocouple junction was mounted in direct contact with the sample and the height to which the sample was raised was adjusted manually to maintain the desired temperature and time duration.

In our cryostat assembly, normally configured for optically detected magnetic resonance studies, it was not possible to attach an aperture mask directly to the sample and still maintain the required ability to raise and lower the sample for *DX* regeneration. Instead, therefore, it was necessary to place a mask smaller than the sample image in front of the detector to insure that only the light transmitted through the sample was being detected. This optical arrangement made it difficult to consistently reproduce optimum optical alignment each time the sample was raised and returned to position. For most of our experiments, this represented no serious problem because the necessary information could be extracted from changes of transmission or MCD versus time or magnetic field, leaving the sample fixed. However, absolute absorption coefficient determinations that required separate measurements of the incident light intensity (by lifting the sample) were therefore less accurate. These limitations will be addressed at the appropriate points in the text which follows.

For transmission measurements, a mechanical chopper (200 Hz) was inserted in the beam before the monochromator, and the transmitted signal was synchronously detected with a lock-in amplifier. For the MCD measurements, 50-kHz alternate left- and right-circular polarization modulation was produced by a linear polarizer and a Hinds International photoelastic modulator placed between the monochromator and the sample. In this case, 50-kHz synchronous detection produced a signal proportional to the difference in the transmitted intensity for left- and right-circular polarizations. The magnetic field was antiparallel to the propagation direction (Faraday configuration). The paramagnetic contribution to the MCD at 1.7 K was estimated by comparison to the MCD measured at 4.2 K, where the $\sim 1/T$ contribution is reduced to only $\sim$25% of its 1.7-K value.

III. THE *DX* METASTABLE STATE

A. Absorption coefficient

The simplest *DX*-center level scheme consists of a ground level, an optical pumping path to a metastable level, and a relaxation barrier. Cooling in the dark populates the ground level, but some electrons may remain trapped at the metastable level, in principle. Then magneto-optical ground-state effects, which might be small, would be inseparable from metastable-state effects, which might be large. Hence, a thorough magneto-optical characterization of the metastable state is first necessary to correctly identify effects exclusive to the ground state.

DX centers were converted to their metastable states by white-light illumination of the sample at 1.7 K. Subsequently, the spectral dependence of the optical-absorption coefficient, α_m, was determined. The transmitted intensities I and I_i, measured with the sample in and out of the beam, respectively, were recorded over a given wavelength range. Then,

$$\alpha_m = -\frac{1}{d}\ln\left[\frac{I}{I_i}\right] + \frac{2}{d}\ln(1-R) , \tag{1}$$

where d is the sample thickness. The second term is the first-order reflection-loss correction (neglecting multiple reflections), which has the value -19.3 cm^{-1} when the reflectivity R at normal incidence is calculated using the index of refraction[31] $n=3.4$.

Figure 1 presents α_m versus wavelength λ. The four data segments correspond to the four different filters used. The offsets between the segments ~ 1 cm^{-1}, correspond to $\sim$4% change in the detected light intensity and serve as a measure of the unavoidable disturbance of the optics in changing filters. Random error in the monochromator starting point causes the glitches since sharp I-vs-λ grating artifacts present in both I and I_i do not completely divide out when evaluating Eq. (1). Fundamental absorption dominates for $\lambda < 0.65$ μm.

A log-log plot of the Fig. 1 data from 0.87 to 2.3 μm gives, for a best fit to the data, $\alpha_m \sim 4.0\lambda^{1.7}$. The wavelength dependence is, therefore, nearly quadratic as predicted by the classical, free-electron, Drude model, which gives[32,33]

$$\alpha_m = \frac{Ne^2}{m^* nc^3 \pi \tau_e}\lambda^2 , \tag{2}$$

where c is the speed of light; n, the index of refraction of the material; e, the electron charge; τ_e, the relaxation time; m^*, the effective mass; and N, the free-carrier concentration. A fit of Eq. (2) to the data yields 3.6 (cm$^{-1}\mu$m^{-2}) for the coefficient of λ^2. This fit is plotted as the smooth curve in Fig. 1.

Equation (2) implies that the absorption is proportional to the total free-carrier concentration. Since the white light used to generate the persistent free-carrier popula-

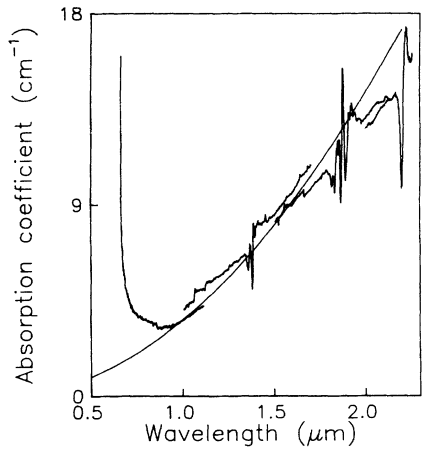

FIG. 1. Absorption spectrum of $Al_{0.35}Ga_{0.65}As$:Te at 1.7 K after white-light bleach.

tion includes photons with sufficient energy to ionize any band-gap level, a significant fraction of the free carriers could originate, in principle, from some bleachable absorber besides the *DX*. To test this, we remeasured α_m after bleaching with monochromatic light at approximately half the band-gap frequency, which still efficiently converts the *DX* (see Sec. IV). Figure 2(a) presents α_m vs λ after a 1.2-μm bleach. Figure 2(b) presents α_m after subsequent additional white-light illumination, which has clearly increased the free-carrier absorption. The difference, Fig. 2(c), reveals that the second contribution comprises about 25% of the total and has similar spectral dependence. Both contributions are similarly persistent, as revealed by a measurement of the transmission after keeping the sample 30 min in the dark subsequent to each bleaching step.

[Note that the values estimated for α_m in Fig. 2(b) are smaller (~ 2.5 cm^{-1}) than those in Fig. 1—even though the data were taken on the identical sample. This serves to illustrate the experimental uncertainty discussed in Sec. II for absolute absorption-coefficient determinations where insertion and removal of the sample from the beam may change the focus and alignment at the detector. The magnitude of this error depends on the optical alignment, which was not identical for the measurements resulting in Figs. 1 and 2, taken on different days. A 5-cm^{-1} error would correspond to an error in the I_0 determination of $\sim 20\%$.]

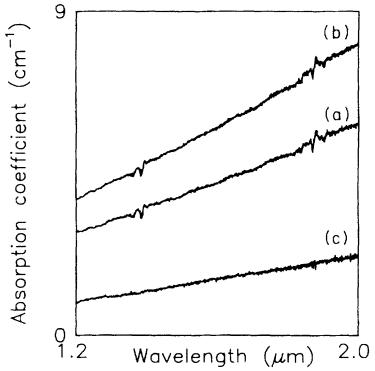

FIG. 2. Absorption spectrum of $Al_{0.35}Ga_{0.65}Te$ at 1.7 K after (a) 1.2-μm-light bleach and (b) subsequent white-light bleach. The difference is given by (c).

B. Magnetic circular dichroism

Next we present our measurements of the MCD of the sample in its bleached state. The measure of MCD, α_{MCD}, defined as $\alpha_L - \alpha_R$ where α_L (α_R) is the absorption for left (right) circularly-polarized light, is determined from the transmitted intensities I_R and I_L according to

$$\alpha_{\mathrm{MCD}} \equiv \alpha_L - \alpha_R \cong \frac{2}{d}\frac{I_R - I_L}{I_R + I_L}, \tag{3}$$

when $(\alpha_L - \alpha_R)d \ll 1$. Here, we monitor simultaneously $I_R - I_L$ from the lock-in output and $I_R + I_L$ directly from the detector with no need to remove the sample. The MCD results are therefore relatively insensitive to the optical alignment and can be more accurately determined than the absolute absorption coefficient.

Figure 3 presents the magnetic-field dependence of the MCD at the wavelengths 0.8 and 1.4 μm after white-light bleaching. A spectrum without the sample shows that the instrumental background circular dichroism is field independent, and we take this as our zero, as shown. The MCD is positive, linear in magnetic field, and increases with wavelength. Measurements at $T = 1.7$ and 4.2 K give identical results within experimental uncertainty, showing that paramagnetism of the metastable state plays an insignificant role in its MCD. Bleaching with 1.2-μm light instead of white light gives similar MCD but with somewhat smaller slopes. This effect will be analyzed quantitatively next.

Figure 4 presents the rate-of-change of MCD with B for $0.9 \leq \lambda \leq 2.0$ μm. These data are slopes from linear fits to curves like those in Fig. 3. Solid triangles represent data taken after bleaching with 1.2-μm light and open squares represent data collected after white-light bleach. The squares tend to lie above the triangles, showing that the additional free carriers generated by white light contribute additional positive MCD. The spectral dependence of the two data sets are similar.

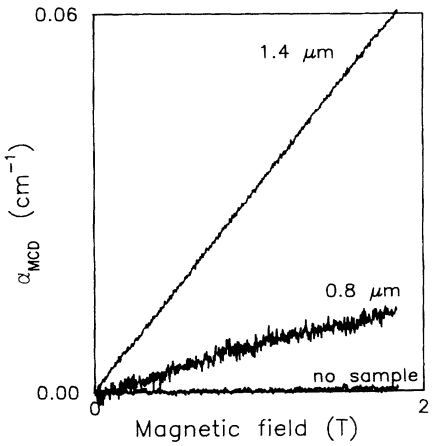

FIG. 3. Field dependence of the MCD at 1.7 K for $Al_{0.35}Ga_{0.65}As$:Te after white-light bleach.

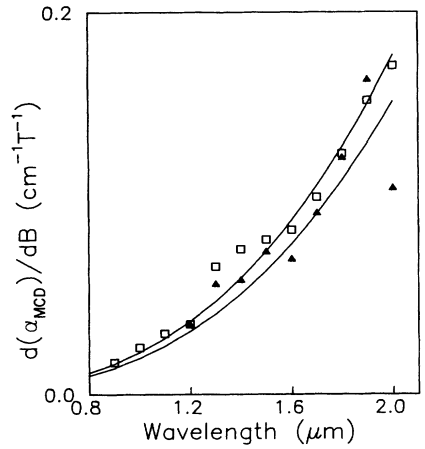

FIG. 4. Spectral dependence of the MCD at 1.7 K for $Al_{0.35}Ga_{0.65}As$:Te after 1.2-μm bleach (solid triangles) and after subsequent white-light bleach (open squares).

Plotting the squares on a log-log plot reveals the power law $\sim\lambda^{2.8}$, an approximately cubic wavelength dependence. Fits of the function $y=c\lambda^3$ to each data set yield the two smooth curves in Fig. 4. The coefficients c for the squares and triangles are 0.0222 and 0.0192 $cm^{-1}\mu m^{-3}T^{-1}$, respectively. Thus, the additional MCD generated by white light comprises approximately 14% of the total.

The results presented in Figs. 3 and 4 have a simple interpretation. The theory of the Faraday effect,[34] using the Drude conductivity tensor, gives the expression

$$\alpha_{\mathrm{MCD}}=\frac{16\pi\sigma_0\omega_c}{nc\tau_e^2\omega^3} \tag{4}$$

for free-carrier MCD. It is proportional to the cyclotron-resonance frequency, $\omega_c=eB/m^*c$, where B is the magnitude of the magnetic field. It is also proportional to the Drude dc conductivity $\sigma_0=Ne^2\tau/m^*$. Care has been taken in determining the sign of Eq. (4) that the relative directions of magnetic field and photon propagation coincide with our experimental situation, and we have adopted the historical optics convention that positive photon-helicity holds for left-circular polarization.[35] The α_{MCD} given by Eq. (4) is positive, linear in the magnetic field, and increases in magnitude as the cube of the wavelength, in agreement with our observations.

Dividing Eq. (4) by Eq. (2) gives

$$\frac{\alpha_{\mathrm{MCD}}}{\alpha_m}=4\frac{\omega_c}{\omega} . \tag{5}$$

Neither N nor τ_e appear, so a comparison of Eq. (5) to our data gives a value for m^*. Equation (5) and the coefficients of the fits to the data in Fig. 1 and the squares in Fig. 3 give $m^*\approx 0.06m_0$. This value agrees reasonably with the value $0.08m_0$ predicted theoretically[36] and verified experimentally[37] for the Γ minimum at an AlAs mole fraction of 0.35. Evidently, the Drude model adequately describes both free-carrier absorption and MCD, despite the perhaps overly simple assumptions of parabolic energy dispersion and a frequency-independent relaxation time.

IV. THE *DX* GROUND STATE

A. Absorption coefficient

After the sample is cooled to 1.7 K in the dark, the optical transmission is found to be strongly time dependent. Figure 5 presents the transmitted intensity versus time for incident light of wavelengths 0.7 and 1.6 μm. The time $t=0$ corresponds to the instant that the shutter is opened and monochromatic light is admitted to the sample. The 0.7-μm transmission asymptotically approaches some final value I_∞, which is more than twice the initial value I_0. This time dependence can be attributed to one or more bleachable absorbers in the sample. The inset presents a semilogarithmic plot of the function $I_\infty-I(t)$ vs time obtained from the 0.7-μm transient. Evidently, the 0.7-μm transient is not a single exponential function of time. This feature will be explained in Sec. IV B.

At 1.6 μm, the transmission decreases exponentially to a saturation value I'_∞. Additional white-light illumination further reduces the transmission to its final value (I_∞). The white light was turned off at $t=700$ s, showing that for a period of 100 s there is no evidence of recovery. The 1.6-μm I'_∞ (I_∞) levels persist unchanged in darkness for 30 min after terminating the 1.6-μm, or subsequent white-light, illumination. These 1.6-μm transmission effects can be attributed to the photogeneration of the two components of persistent free-carrier absorption (Fig. 2).

Figure 5 shows also that the transient rate is slower at the longer wavelength. For $\lambda>1.6$ μm, the rates become so slow that the final state is not obtained in experimentally convenient times. Additional illumination with 1.2 $\mu m<\lambda<1.6$ μm light was therefore used to more rapidly determine the final unchanging transmission level I'_∞. Subsequent white-light illumination induces a further transmission decrease to the level I_∞ that is stable at all wavelengths. As before, each induced transmission change is persistent.

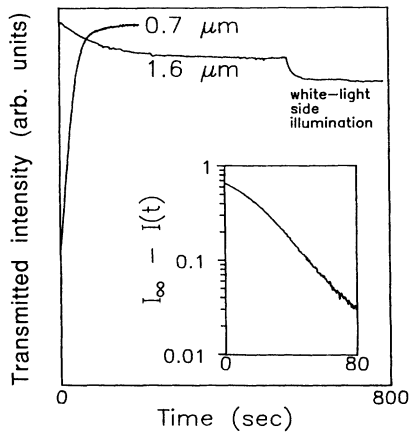

FIG. 5. Examples of transmission transients observed after cooling $Al_{0.35}Ga_{0.65}As$:Te to 1.7 K in the dark. The effect of white-light side illumination on the long-wavelength transient is also shown. The inset is a semilogarithmic plot of the 0.7-μm transient.

If bleachable absorbers, initially in their ground states, are completely converted to the metastable (free-carrier) state, then the difference between ground- and metastable-state absorption coefficients is

$$\alpha_g - \alpha_m = -\frac{1}{d}\ln\left[\frac{I_0}{I_\infty}\right] . \quad (6)$$

Again, this is accurately determined because all time-independent absorption in the sample, the intensity of the incident light, and the spectral dependence of the optics and detector divide out. The intensity I_∞ was taken as the transmitted intensity after white-light illumination, which was determined at the end of the run at each wavelength.

The open circles in Fig. 6 represent values for the difference $\alpha_g - \alpha_m$, found from measured transients and Eq. (6), as a function of wavelength. The difference is large and positive at short wavelengths, showing that here $\alpha_g \gg \alpha_m$.

For $\lambda > 1.5$ μm, $\alpha_g < \alpha_m$ and the data of Fig. 6 approach the average of the two solid curves, which represent independent measured estimates of $-\alpha_m$. The long smooth curve is the function $-4\lambda^{1.7}$ found to fit the data presented in Fig. 1. The short smooth curve is the negative of the Fig. 2(b) curve. In the last paragraph of Sec. III A, we attributed the difference in the two smooth curves to a specific experimental limitation, which does not affect the measurements resulting in the open circles. We conclude that α_g is nearly zero for all bleachable absorbers when $\lambda > 1.7$ μm.

If we add values for α_m to the values for $\alpha_g - \alpha_m$ represented by open circles in Fig. 6, then we obtain the absorption coefficient α_g for transitions from the ground levels of the *DX* and other bleachable absorbers. Using a simple parabolic function $\alpha_m = 2.5\lambda^2$ to represent an average of the two smooth curves plotted in Fig. 6, we obtain the open circles presented in Fig. 7. At long wavelength, α_g approaches zero. In going toward short wavelength the data continuously rise to a $\sim 30\text{-cm}^{-1}$ plateau between 0.7 and 0.8 μm. At 0.66 μm, α_g has the value $\sim 60\ \text{cm}^{-1}$, revealing an abrupt rise in absorption. It was not possible to probe the sample with even shorter wavelengths because the rapidly rising fundamental absorption made the transmission immeasurably small.

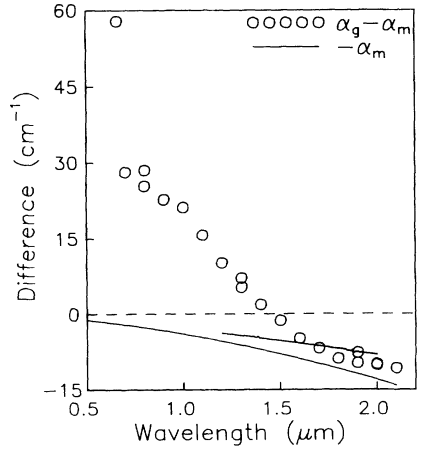

FIG. 6. Spectral dependence of $\alpha_g - \alpha_m$. The smooth curves represent separate and independent measurements of $-\alpha_m$. The dashed line denotes the ordinate zero.

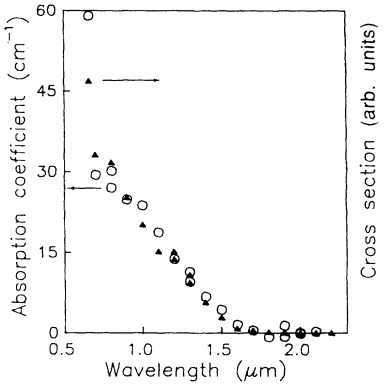

FIG. 7. Spectral dependence of the ground-state absorption coefficient and the optical-conversion cross section for bleachable absorbers in $Al_{0.35}Ga_{0.65}As$:Te at 1.7 K. Values for $\alpha_g(\sigma)$ are given by open circles (solid triangles).

B. Conversion cross section

The results of Sec. IV A represent, to our knowledge, the first direct transient transmission measurement of the optical-absorption coefficient of the deep bleachable absorbers in $Al_xGa_{1-x}As$. Previously, it has been primarily the cross section σ for optical ground- to metastable-state conversion that has been measured and assumed to have the same spectral dependence as the absorption coefficient. We can now test this, since

$$\sigma = (\tau\phi)^{-1} , \quad (7)$$

where the conversion rate, τ^{-1}, and a relative measure of the photon flux ϕ, are also obtained in our experiment.

The conversion rate τ^{-1} is found simply from the slope of $\ln|I_\infty - I(t)|$ vs t obtained from the pure exponential transients found at wavelengths longer than about 1 μm. For $\lambda \leq 1$ μm, the transients are nonexponential, as demonstrated by the inset of Fig. 5, where the initial conversion rate is apparently lower than the final rate. This effect can be explained as arising from a nonuniform-intensity distribution within the sample, since for $\lambda \leq 1$ μm, $\alpha_g d > 1$. In order to analyze this, we model the time-dependent transmission which occurs when a sample contains a strong, bleachable absorber. The equation that describes the transmitted flux $\phi(x=d, t)$ as photons eat their way through from $x=0$ to the back of the sample at $x=d$ is

$$\phi(d,t) = \phi(x=0)\exp\left[-(\alpha_g - \alpha_m) \times \int_0^d \exp\left[-\sigma\int_0^t \phi(x,t)dt\right]dx\right] . \quad (8)$$

With $(\alpha_g - \alpha_m)$ determined by the ratio

$\phi(d,0)/\phi(d,\infty)=I_0/I_\infty$ as given by Eq. (6), we find that each nonexponential transient can be accurately reproduced by a suitable choice of σ.

The solid triangles in Fig. 7 give our values of σ vs λ where for $\lambda \leq 1$ μm, σ is found from the fit of Eq. (8) to the measured transmission transients. (The σ data have been multiplied by a single scaling factor so that they may be plotted over the same ordinate range as the α_g data.) It is clear that both σ and α_g have the same spectral dependence, and this confirms that the optical-absorption cross section and the optical conversion cross section are, indeed, proportional.

Since τ^{-1} can be estimated accurately for values ranging from a few seconds to many minutes, accurate values of σ can be obtained over many decades and extend, therefore, over a much wider spectral range than available for the absorption coefficient. Figure 8 presents the spectral dependence of $\log_{10}\sigma$ (solid triangles) over six decades. The solid line (suitably scaled from Fig. 4 of Ref. 3) is the *DX* conversion cross section found in $Al_{0.37}Ga_{0.63}As$:Te by a capacitance-transient technique. The spectral dependence of the triangles and line agree well for $\lambda \geq 0.9$ μm, confirming that here our transients reflect the well-established *DX* conversion only. For $\lambda \leq 0.8$ μm, however, the data and curve diverge significantly, revealing the onset of a second, more rapidly bleaching absorber. The sudden increase in α_g at 0.66 μm (Fig. 7) also supports this identification of a second bleaching process in this spectral region.

In order to better characterize the second bleaching process, we performed the following double-bleaching experiment. After cooling the sample in the dark, the *DX* center was first bleached with monochromatic light at 1.2 μm, where we are reasonably sure that only the *DX* is being bleached. Then, the sample transmission at shorter wavelengths was monitored to see if any other bleachable absorption remained. Figure 9 presents the sample transmission versus time where, at $t=0$, the shutter is opened and 1.2-μm monochromatic light is admitted to the sample. The 1.2-μm transmission rises exponentially to a stable level, the shutter is closed, and the monochromator is quickly set to 0.66 μm. Upon reopening the shutter, a second transient is observed. Afterward, no

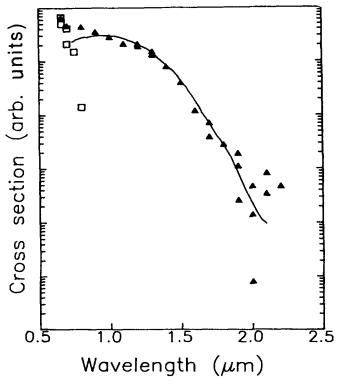

FIG. 8. Spectral dependence of the conversion cross section for *DX* (solid triangles) and PPC2 (open squares). The smooth curve was taken from Fig. 4 of Ref. 3.

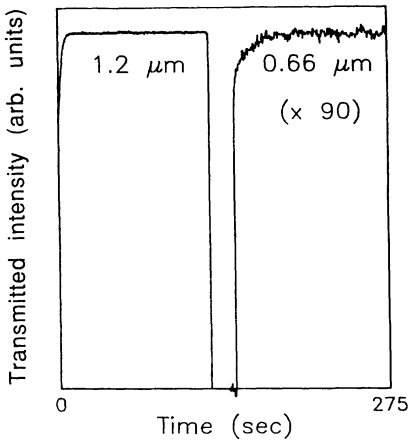

FIG. 9. Separated *DX* and PPC2 transmission transients.

further transmission change at any wavelength can be induced by white-light side illumination.

Values for the conversion cross section of the second bleaching process, obtained in this manner according to Eq. (7), are plotted versus wavelength as the open squares in Fig. 8. The squares and triangles match at $\lambda=0.66$ μm, but the squares fall off rapidly with increasing wavelength. Evidently, the second process is insignificant at the longer wavelengths where the triangles match the smooth curve. Since bleaching the second, short-wavelength band generates additional persistent photoconductivity (Sec. III), we identify the second transient with PPC2.

C. Metastable- to ground-state recovery

The metastable- to ground-state recovery for *DX* and PPC2 was measured by monitoring the partial recovery of their corresponding $I_0 \rightarrow I_\infty$ transmission transients after isochronal and isothermal sample anneals at intermediate temperatures, with the following results: When the sample is warmed to an insufficiently high temperature and then recooled in the dark, the bleached centers do not return to their ground states, no transient is observed, and $\ln(I_0/I_\infty)$ is zero. When the sample is warmed above ~ 100 K, we find transients similar to those in Fig. 9, and $\ln(I_0/I_\infty)$ has its maximum value, $[\ln(I_0/I_\infty)]_{\max}=-d(\alpha_g-\alpha_m)$ for both *DX* and PPC2. In Fig. 10, we present $\ln(I_0/I_\infty)/[\ln(I_0/I_\infty)]_{\max}$ after five-minute isochronal anneals as a function of annealing temperature. The open circles are found from the initial 1.2-μm transients associated with the *DX*. The solid squares are found from the subsequent 0.66-μm transients associated with PPC2. Recovery of PPC2 occurs at a temperature about 10 K lower than does recovery of the *DX*.

Figure 11 presents isothermal annealing data for the *DX* and PPC2. Here we plot the function $1-\{\ln(I_0/I_\infty)/[\ln(I_0/I_\infty)]_{\max}\}$. When no transient is observed, this function has the value 1. Following complete recovery, where the full transient is observed, it has the value 0. The top portion of Fig. 11 presents the data for the *DX* and the lower portion presents the data for PPC2. The data corresponding to different annealing

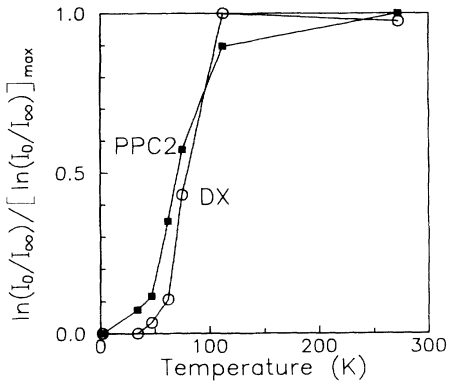

FIG. 10. Normalized magnitude of the transmission change after 5-min isochronal anneals for the *DX* (open circles) and PPC2 (solid squares).

temperatures are labeled and distinguished by different symbols. All the recovery curves are highly nonexponential. For the *DX* at the temperatures 60 and 65 K, the behavior may be characterized by a rapid partial recovery during the first few seconds of the anneal followed by changes that are small compared to the scatter in the data. At higher temperatures the nonexponentiality is similar to what has been observed by many workers since the earliest[38] Hall measurements of *DX* PPC decay. A careful study of decay data over the broader range of temperatures studied here has also recently been published.[39]

The degree of recovery for PPC2 at 60 K is about the same as that for the *DX* at 70 K, confirming the PPC2 begins its recovery at a temperature approximately 10 K lower than does the *DX*. The scatter in the data is considerably larger for PPC2 than for the *DX*, since the transmission signal level is about 100 times smaller at 0.66 μm than at 1.2 μm. This is due to a combination of

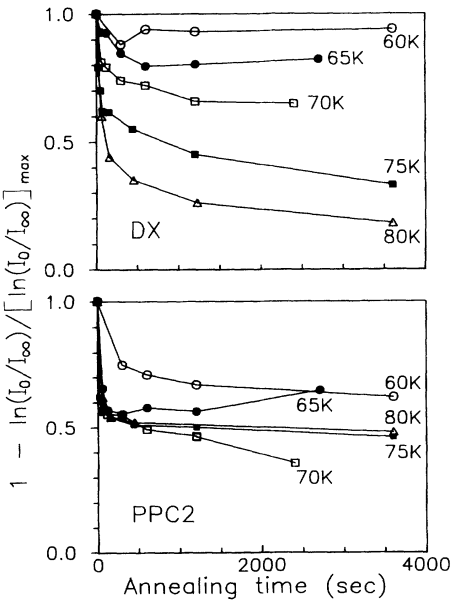

FIG. 11. Transmission transient recovery for isothermal anneals of *DX* (top) and PPC2 (bottom).

reduced source-monochromator efficiency and strong fundamental absorption at 0.66 μm. Nonetheless, it is clear that the recovery behavior is fundamentally different for PPC2 than for the *DX*. In particular, over a wide temperature range, PPC2 recovery seems to proceed rapidly to a level of about 50%, where it apparently becomes locked.

D. Magnetic circular dichroism

Like the transmission, the MCD is also found to be time dependent after cooling the sample in darkness, but it differs from the transmission by being magnetic-field dependent. The exploration of this field dependence requires the measurement of many transients, and the sample must be warmed above 100 K and recooled in the dark each time. As for the transmission measurements, this is accomplished by raising the sample up into the warm cyrostat neck ($T \approx 250$ K) and then lowering it again into the liquid helium. Small shifts in optical alignment result every time this is done, and this produces shifts in the background instrumental circular dichroism.

Fortunately, we again have a systematic way to eliminate the instrumental background so that its random shifts do not introduce experimental uncertainty to the transient MCD measurements. $\alpha_{MCD}(t)$ always increases to a steady state $\alpha_{MCD}(\infty)$, identified as the free-carrier MCD (Sec. III B), whose field dependence is well characterized (Fig. 3). We measure $\alpha_{MCD}(t)$ until it has stopped changing. Then, leaving the optical alignment undisturbed, the field is ramped down while monitoring the linear decrease of $\alpha_{MCD}(\infty)$. Its value $B=0$ is the instrumental background, which we subtract from $\alpha_{MCD}(t)$.

Examples of $\alpha_{MCD}(t)$ measured at 0.9 μm for field strengths of 0 and 1.9 T are presented in Fig. 12. As expected at $B=0$, $\alpha_{MCD}(t)$ is constant and defines our zero. At 1.9 *T*, $\alpha_{MCD}(t)$ increases from an initially finite, positive value to its steady-state, free-carrier value $\alpha_{MCD}(\infty)$. The initial MCD can be identified with transitions from the ground levels of the *DX* and PPC2. This will be justified more fully next.

Figure 13 gives the initial MCD for wavelengths 900,

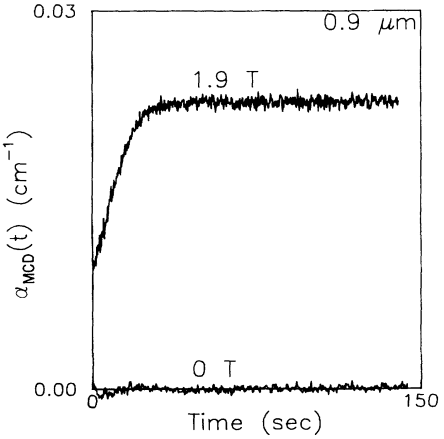

FIG. 12. Transient MCD at 0.9 μm after cooling $Al_{0.35}Ga_{0.65}As$:Te to 1.7 K in the dark.

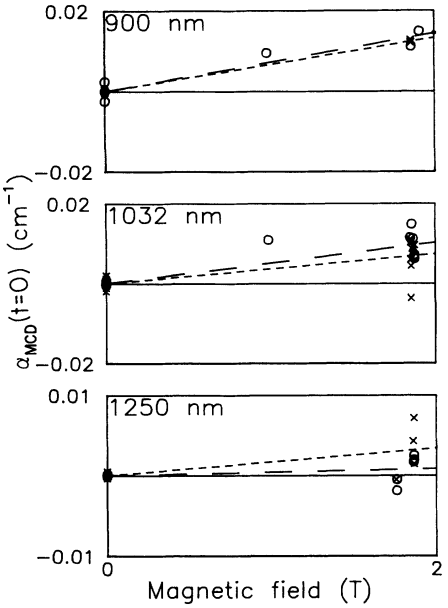

FIG. 13. Initial MCD vs magnetic field at 900, 1032, and 1250 nm. Data measured at 1.7 K (4.2 K) are given by open circles (crosses) and fit by dashed (dotted) lines.

1032, and 1250 nm. These wavelengths were chosen to probe the broad absorption band near its peak and maximum derivative positions, the regions where maximum MCD is normally encountered. The circles (crosses) are 1.7 K (4.2 K) data. The dashed (dotted) lines are linear fits to the 1.7 K (4.2 K) data. The initial MCD decreases rapidly with increasing wavelength, opposite to the free-carrier MCD spectral dependence (Fig. 4), so any free-carrier contribution to the initial MCD is small. This supports our identification of the initial MCD with transitions only from the ground states of the *DX* and PPC2.

The initial MCD shows no statistically significant temperature dependence. Values of the initial MCD at 2 T for the temperatures 1.7 and 4.2 K are given in Table I. Their difference at each wavelength, also given in Table I, is a measure of the scatter and gives an upper limit for possible paramagnetic contributions to the MCD. Dividing this difference at 0.9 μm, where the ground-state MCD is largest, by $\alpha_g \sim 30$ cm^{-1} shows that the paramagnetic contribution to the fractional MCD is less than 0.004%.

V. SUMMARY AND CONCLUSIONS

In Sec. III A we presented absorption spectra for our $Al_{0.35}Ga_{0.65}As$:Te sample when the *DX* centers, or the *DX* together with a second bleachable absorber (PPC2), were in their metastable states. An adequate description was provided by the Drude free-electron model. Previous measurements[40] of *DX* metastable-state absorption spectra from 3.3 to 25 μm for more lightly doped ($1-4\times10^{16}$ cm^{-3}) $Al_xGa_{1-x}As$:Te at 10 K have been interpreted as the photoionization tail of a shallow level. Our measurements extend the previous results to higher-frequency and greater-carrier concentration, where the free-electron model might be expected to provide a reasonable description.

Recent measurements[41] from 0.62 to 2.5 μm on optically thick $Al_{0.46}Ga_{0.54}As$:Te at 77 K under constant 1.06 μm illumination, or in thermal equilibrium at 300 K, revealed a broad peak at 2.2 μm superimposed on a free-carrier absorption background. Our wavelength range is too limited to be able to identify such a peak in our spectra (Fig. 1). The peak was interpreted as evidence for an intracenter transition to an excited state of the *DX*, but there is an alternative possible explanation. A broad peak superimposed on free-carrier absorption has been found at similar wavelengths in the spectra of *n*-type, GaP,[42] GaP_xAs_{1-x},[43] GaAs,[44,45] InP,[46] GaSb,[47] AlSb,[32] and Si,[48] and is attributed in each case to excitation of free electrons from the conduction-band minimum to secondary minima. Peaks in free-carrier absorption can also occur, in principle, when optical-deformation potential scattering is dominant.[49]

Reference 41 also showed that at 77 K long-wavelength (free-carrier) absorption disappeared with a 10 s time constant after terminating the illumination, while the short-wavelength (*DX*-band) absorption showed only a 50% recovery during this time. The interpretation[41] was that recapture of free carriers takes place via some intermediate, localized state. Invoking the negative-*U* model,[14,15] this state was identified as the neutral charge state of the *DX*. Our Fig. 11, which shows a rapid 50% recovery of transmission transients in the 77-K range but only a slow full recovery, is consistent with the experimental observations of Ref. 41. Since we did not monitor the longer-wavelength free-carrier recovery separately, we cannot confirm or deny their interpretation.

In Sec. III B we presented measurements of the sample's MCD when the *DX*, or the *DX* together with PPC2, were in their metastable states. The results were interpreted by the theory of the Faraday effect and were again found to be adequately described by the free-electron Drude model. Furthermore, a comparison of the absorption coefficient and the MCD yielded a value for the electron effective mass which was in reasonable agreement with a recent, more accurate report.

In Sec. IV A we described the transmission transients observed after cooling the sample to 1.7 K in the dark. Values for the difference in ground- and metastable-state absorption coefficients for the *DX* and PPC2 together were obtained from the initial and final transmission levels. Then, using the results of Sec. III A, we arrived at values for the ground-state absorption coefficient alone. This represents, to our knowledge, the first direct transient transmission measurement of the optical-absorption

TABLE I. Initial MCD (2 T) from 1.7 and 4.2 K data and difference.

Wavelength (nm)	Initial MCD at 2 T (cm^{-1}) 1.7 K	4.2 K	Difference (cm^{-1})
900	0.014 4	0.013 3	0.001 10
1032	0.010 3	0.007 46	0.002 84
1250	0.000 84	0.003 40	−0.002 56

coefficient of the deep bleachable absorbers in $Al_xGa_{1-x}As$. This absorption was found to approach zero at long wavelength, but near the band gap the absorption rose abruptly to a large value.

In Sec. IV B, we presented our determination of the optical-conversion cross sections for the bleachable absorption processes. We found that the conversion cross section for the *DX* and PPC2 together has the same spectral dependence as their ground-state absorption coefficient. The conversion threshold is about 0.6 eV for the *DX* and about 1.5 eV for PPC2.

Our measurement (Sec. IV C) of the metastable- to ground-state recovery of the *DX* and PPC2, separately, revealed significant differences between the two. This difference, together with the large difference in optical ionization threshold, suggest that the *DX* and PPC2 are unrelated. Following our optical identification of PPC2, Mochizuki and Mizuta[50] have observed it via photo-Hall measurements in a specimen cut from the same wafer as our sample. These workers found no evidence of PPC2 in molecular-beam-epitaxy material, however. Hence, we tentatively conclude that PPC2 is related to another interesting defect that displays *DX*-like behavior, but one that is apparently specific to our sample and that it is therefore unrelated to the Te *DX* center.

In Sec. IV D we presented measurements of the time-dependent MCD. The initial MCD showed no evidence of a free-carrier contribution. Contributions from nonbleaching centers must be small also; otherwise the simple free-carrier interpretation for the metastable state (Sec. III) would have been inadequate. Hence, we were able to identify the initial MCD with optical transitions originating in the *DX* and PPC2 ground levels.

The initial MCD shows no statistically significant temperature dependence. Taking the scatter as an upper limit for the possible paramagnetic contribution to the *DX* ground-state MCD, a value of only 0.004% of the absorption coefficient is found. Since fractional MCD (scaled to our temperature and field strength) of paramagnetic defects in semiconductors or insulators is usually[51–55] on the order of 0.1–10 %, our result supplies strong additional support to the diamagnetic-ground-state, negative-*U* model of Chadi and Chang.[14,15]

It is important to point out, however, that it is not a *proof*. As pointed out in the introduction, the *detection* of a significant paramagnetic contribution would have served as a proof for a paramagnetic ground state. However, as in EPR, the *failure* to detect paramagnetism is not a proof of its absence. In the case of MCD, its strength is proportional to spin-orbit interaction in the final level of the optical-absorption transition. We have no direct information of its magnitude and it could be small and strongly quenched by the low symmetry of the defect. Thus, the very low upper limit that we have established for the paramagnetic MCD component must be considered another strong evidence against the neutral, paramagnetic, single-electron-state model, but this latter model is still not completely ruled out and therefore continues to deserve scrutiny in future works.

ACKNOWLEDGMENTS

This work was supported by National Science Foundation Grant No. DMR-89-02572. In addition, one of us (Y.M.) would like to acknowledge M. Mizuta for fruitful discussions, and is also grateful to F. Saito, H. Watanabe, M. Ogawa, and Y. Wada for encouragement and support.

*Present address: Fundamental Research Laboratories, NEC Corporation, 34, Miyukigaoka, Tsukuba, Ibaraki 305, Japan.

[1]D. V. Lang, in *Deep Centers in Semiconductors,* edited by S. T. Pantelides (Gordon and Breach, New York, 1986), pp. 489–539.

[2]P. M. Mooney, J. Appl. Phys. **67**, R1 (1990).

[3]D. V. Lang, R. A. Logan, and M. Jaros, Phys. Rev. B **19**, 1015 (1979).

[4]M. Mizuta, M. Tachikawa, H. Kukimoto, and S. Minomura, Jpn. J. Appl. Phys. **24**, L143 (1985).

[5]G. A. Northrup and P. M. Mooney, J. Electron. Mater. **20**, 13 (1991).

[6]V. Narayanamurti, R. A. Logan, and M. A. Chin, Phys. Rev. Lett. **43**, 1536 (1979).

[7]T. Kitano and M. Mizuta, Jpn. J. Appl. Phys. **26**, L1806 (1987).

[8]M. Mizuta and T. Kitano, Appl. Phys. Lett. **52**, 126 (1988).

[9]T. M. Hayes, D. L. Williamson, A. Outzourhit, P. Small, P. Gibart, and A. Rudra, J. Electron. Mater. **18**, 207 (1989).

[10]P. Gibart, D. L. Williamson, B. El Jani, and P. Basmaji, Phys. Rev. B **38**, 1885 (1988).

[11]P. Gibart, D. L. Williamson, B. El Jani, and P. Basmafi, in *Proceedings of the Fourteenth International Symposium on GaAs and Related Compounds,* edited by A. Christou and H. S. Rupprect, IOP Conf. Proc. No. 91 (Institute of Physics and Physical Society, London, 1988), p. 377.

[12]K. M. Yu, K. Khachaturyan, E. R. Weber, H. P. Lee, and E. G. Colas, Phys. Rev. B **43**, 2462 (1991).

[13]J. E. Rowe, F. Sette, S. J. Pearton, and J. M. Poate, in *Physics of DX Centers in GaAs Alloys,* edited by J. C. Bourgoin, Solid State Phenomena Vol. 10 (Sci Tech Publications, Liechtenstein, 1990), p. 283.

[14]D. J. Chadi and K. J. Chang, Phys. Rev. Lett. **61**, 873 (1988).

[15]D. J. Chadi and K. J. Chang, Phys. Rev. B **39**, 10366 (1989).

[16]G. D. Watkins, in *Festkörperprobleme (Advances in Solid State Physics),* edited by P. Gross (Vieweg, Braunschweig, 1984), Vol. XXIV, p. 163.

[17]J. Dabrowski, M. Scheffler, and R. Strehlow, in *The Physics of Semiconductors Vol. I,* edited by E. M. Anastassakis and J. D. Joannopoulos (World Scientific, Singapore, 1990), p. 489.

[18]E. Yamaguchi, K. Shiraishi, and T. Ohno, in *The Physics of Semiconductors Vol. I* (Ref. 17), p. 501.

[19]G. D. Watkins, Semicond. Sci. Technol. **6**, B111 (1991).

[20]P. W. Anderson, Phys. Rev. Lett. **34**, 953 (1975).

[21]P. Gibart, D. L. Williamson, J. Moser, and P. Basmaji, Phys. Rev. Lett. **65**, 1144 (1990).

[22]J. A. Wolk, M. B. Kruger, J. N. Heyman, W. Walukiewicz, R. Jeanloz, and E. E. Haller, Phys. Rev. Lett. **66**, 774 (1991).

[23]T. Fujisawa, J. Yoshino, and H. Kukimoto, Jpn. J. Appl. Phys. **29**, L388 (1990).

[24]K. A. Khachaturyan, D. D. Awschalom, J. R. Rozen, and E.

R. Weber, Phys. Rev. Lett. **63**, 1311 (1989).
[25]S. Katsumoto, N. Matsunaga, Y. Yoshida, K. Sugiyama, and S. Kobayashi, Jpn. J. Appl. Phys. **29**, L1572 (1990).
[26]H. J. von Bardeleben, M. Zazoui, and S. Alaya, Phys. Rev. B **42**, 1500 (1990).
[27]P. M. Mooney, W. Wilkening, U. Kaufmann, and T. F. Kuech, Phys. Rev. B **39**, 5554 (1989).
[28]D. K. Maude, L. Eaves, T. J. Foster, and J. C. Portal, Phys. Rev. Lett. **62**, 1922 (1989).
[29]D. J. Chadi, K. J. Chang, and W. Walukiewicz, Phys. Rev. Lett. **62**, 1923 (1989).
[30]C. H. Henry and C. P. Slichter, in *Physics of Color Centers,* edited by W. Beall Fowler (Academic, New York, 1968), pp. 384–403.
[31]M. Guzzi and J. L. Staehli, in *Physics of DX Centers in GaAs Alloys,* edited by J. C. Bourgoin, Solid State Phenomena Vol. 10 (Ref. 13), p. 25.
[32]W. J. Turner and W. E. Reese, Phys. Rev. **117**, 1003 (1960).
[33]H. Y. Fan and M. Becker, in *Proceedings of the Reading Conference on Semiconducting Materials,* edited by H. K. Henisch (Butterworths, London, 1951), pp. 132–147.
[34]J. G. Mavroides, in *Optical Properties of Solids,* edited by F. Abeles (Elsevier, New York, 1972), p. 351.
[35]J. D. Jackson, *Classical Electrodynamics,* 2nd ed. (Wiley, New York, 1975), p. 274.
[36]J. W. Harrison and J. R. Hauser, J. Appl. Phys. **47**, 292 (1976).
[37]T. Inoshita and N. Iwata, Phys. Rev. B **42**, 1296 (1990).
[38]R. J. Nelson, Appl. Phys. Lett. **31**, 351 (1977).
[39]J. Y. Lin, A. Dissanayake, G. Brown, and H. X. Jian, Phys. Rev. B **42**, 5855 (1990).
[40]J. E. Dmochowski, J. M. Langer, and J. Raczynska, Phys. Rev. B **38**, 3276 (1988).
[41]Y. Mori, T. Yokota, and H. Ohkura (unpublished).
[42]W. G. Spitzer, M. Gershenzon, C. J. Forsch, and D. F. Gibbs, J. Phys. Chem. Solids **11**, 339 (1959).
[43]J. W. Allen and J. W. Hodby, Proc. Phys. Soc. London **82**, 315 (1962).
[44]W. G. Spitzer and J. M. Whelan, Phys. Rev. **114**, 59 (1959).
[45]I. Balslev, Phys. Rev. **173**, 762 (1968).
[46]M. R. Lorenz, W. Reuter, W. P. Dumke, R. J. Chicotka, G. D. Pettit, and J. M. Woodall, Appl. Phys. Lett. **13**, 421 (1968).
[47]W. M. Becker, A. K. Ramdas, and H. Y. Fan, J. Appl. Phys. **32**, 2094 (1961).
[48]W. G. Spitzer and H. Y. Fan, Phys. Rev. **108**, 268 (1957).
[49]K. Seeger, *Semiconductor Physics, An Introduction,* 4th ed. (Springer-Verlag, New York, 1989), p. 350.
[50]Y. Mochizuki and M. Mizuta (private communication).
[51]K. Sato, T. Iijima, T. Nakajima, K. Yahagi, and S. Kobayashi, Jpn. J. Appl. Phys. **27**, 979 (1988).
[52]F. J. Ahlers, F. Lohse, J. M. Spaeth, and L. F. Mollenauer, Phys. Rev. B **28**, 1249 (1983).
[53]D. M. Hofmann, F. Lohse, H. J. Paus, D. Y. Smith, and J. M. Spaeth, J. Phys. C **18**, 443 (1985).
[54]F. A. Modine and E. Sonder, J. Phys. C **7**, 204 (1974).
[55]F. A. Modine, Y. Chen, R. W. Major, and T. M. Wilson, Phys. Rev. B **14**, 1739 (1976).